CONCRETE RESEARCH LETTERS

www.crl.issres.net Vol. 5 (4) – 2014

Experimental and FE simulations of Ferrocement Domes Reinforced with Composite Materials

Yousry B.I. Shaheen[1], Boshra A. Eltaly [2], Amany A. Hanesh[3]

[1]Professor of Strength and Testing of Materials, Faculty of Engineering, Minufiya University, EGYPT

[2]Lecturer in Department of Civil Engineering, Faculty of Engineering, Minufiya University, EGYPT

[3]M. Sc. student. Civil Engineering Department, Minufiya University, EGYPT

Received: 20/08/2014 – Revised 20/11/2014 – Accepted 1/12/2014

Abstract

The main objective of the current researches is estimating the structure performance of ferrocement domes reinforced with composite material. The current paper presented an experimental program included casting and testing up to failure for four ferrocement domes. All specimens have 1000 mm diameter and 500 mm height; respectively and they were reinforced with welded wire meshes (for the first and second dome), fiberglass meshes (for the third dome) and polyethylene wire meshes (for the fourth dome). The second dome is the same as the first dome except that the second dome has two opening with 100 x 100 mm dimensions to indicate the effect of the opening in the structure behavior of ferrocement dome. Also FE simulations for all tested domes were employed. The results of the experimental program indicated that the dome reinforced with fiberglass mesh has the highest service load and ultimate load and the dome reinforced with welded wire meshes achieved highest ductility ratio and energy absorption. Additionally comparing the results of FE simulations with the experimental results showed that the results of FE simulation is closed the experimental results.

Keywords: Ferrocement; Fiberglass mesh; Polyethylene mesh; Cracking; Ductility; Finite element simulation; Nonlinear analysis.

1. Introduction

Ferrocement concrete, large amounts of small-diameter wire meshes are used instead of reinforcing bars and in which Portland cement mortar is used instead of concrete in the reinforced concrete. Ferrocement is reinforced with a wide variety of metallic reinforcing mesh materials; woven wire mesh, welded wire mesh and expanded metal mesh. Ferrocement has been used for at least 150 years in construction the boat building. Due to the many researches that were conducted on ferrocement technology, recently the applications of ferrocement have become versatile such as different roofing systems, retaining walls, sculptures, bus shelters, bridge decks, repair works, water structures like tanks, strengthening and precast ferrocement elements (1-6).

Many investigators have reported the advantages of ferrocement in comparing with the conventional reinforced concrete. Also numerous test data are available to define its performance criteria for construction and repair of structural elements. From these investigations, it can be concluded that ferrocement has features included ease of prefabrication and low cost in maintenance and repair. Compared with the conventional reinforced concrete, ferrocement is reinforced in two directions (with wire meshes) so that it has homogenous-isotopic properties in the two directions. Also ferrocement generally has a high tensile strength and a high modulus of rupture because that it usually benefits with its high reinforcement ratio. Additionally, because the specific surface of reinforcement of ferrocement is one to two orders of magnitude higher than that of reinforced concrete, larger bond forces develop with the matrix resulting in average crack spacing and width more than one order of magnitude smaller than in conventional reinforced concrete [7-14]. The application of Ferrocement to the dome structure has made it possible to construct alight but strong, durable weather resistant shell with a weight reduction to almost 1/10th of the conventional material [15-18].

Verious studies were carried out to study the structural behavior of reinforcement concrete elements reinforced with new composite materials such as fiberglass, FRP, GFRP and PVC. The results of the Daniel and Shah [19] and Al-sayed and Al-hozaimy [20] studies indicated that fiberglass has excellent corrosion resistance, high tensile strength, high degree of flexibility and good non-magnetization properties. Also Harris et al. [21] experimental results that were carried out on beams reinforced with hybrid FRP reinforcing bars indicated that the ductility index of these beams were close to that of the beams reinforced with steel bar. Li and Wang [22] and Zhang and Huang [23] tested concrete beams reinforced with GFRP and steel bars to estimate thier flexural behavior and their results showed that the beam reinforced with GFRP has the best flexural behavior. Sakthivel and Jagannathan [24] investigated a new non-corrosive mesh material in ferrocement; PVC-coated steel welded mesh. Then Sakthivel and Jagannathan [25] studied a low-velocity impact study on square fibrous ferrocement slab (250mm length and 25mm thickness) reinforced with PVC-coated welded mesh. Their results indicated that the impact energy increases with increasing in the number of mesh layers. Hafiz [26] and Shaheen et al. [27] studied the structural behavior of fourteen ferrocement channel beams under four point loadings until failure. The beams reinforced with various types of meshes; welded, expanded and fiberglass meshes. Their results indicated that the beam reinforced with welded wire mesh achieved higher first crack load, serviceability load, ultimate load and energy absorption than beams reinforce with expanded and fiberglass mesh. Abdul-Fataha [28] and Shaheen et al. [29] designed an experimental program and employed numerical models to examine the structural behavior of twelve ferrocement beams under three point loadings up to failure. The twelve beams were different in the type of reinforcements; steel bars, traditional wire meshes (welded and expanded wire meshes) and composite materials (fiberglass wire meshes and polypropylene wire meshes). The results of the experimental tests and numerical models concluded that the beam with fiber glass meshes gives the lowest first crack load and ultimate load. Also their results indicated that the ferrocement beam reinforced with four layers of welded wire meshes has better structural behavior than those beams reinforced with other types of wire meshes.

The current research presents the results of experimental program that was designed to examine the structure performance of four ferrocment domes. These dome reinforced with metal wire meshes; welded wire meshes and non-metal wire meshes (composite material); fiberglass meshes and polyethylene wire meshes. The experimental results of the four tested domes comprised load-vertical and horizontal curves, crack patterns, first crack load, ultimate load, service load, energy absorption and ductility ratio. Also in the current work, all the tested domes were simulated by finite element ANSYS program and the results of the Finite Element (FE) simulations were to investigate their flexural behavior up to failure.

2. Experimental work

The current experimental program includes casting and testing four spherical domes; D1, D2, D3 and D4. The diameter and the height of all specimens were 1000 mm and 500 mm;

respectively. The thickness of the domes was different because of the requirements of the construction method. The thickness of D1 and D2 were 50mm and the thickness of D3 and D4 were 60 mm. The first, third and the fourth dome were cast without opening and the second dome was cast with two opening with 100 x 100 mm dimensions as shown in Figure 1. All the details of the tested domes are indicated in Table 1.

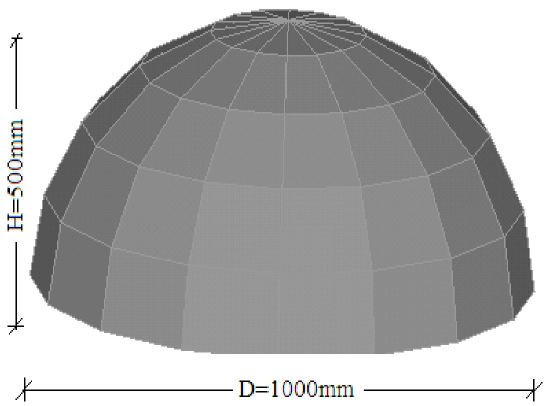

a) Without opening

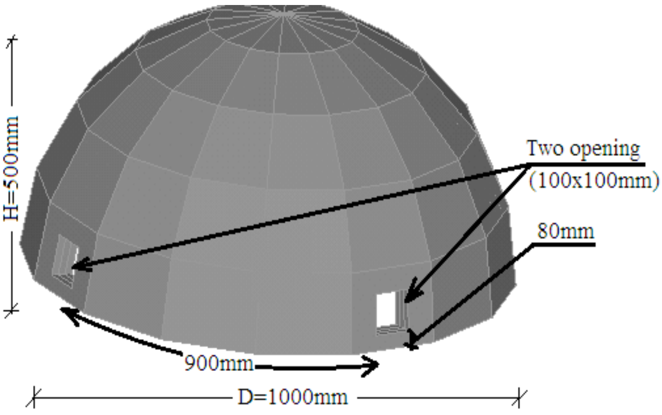

b) With two openings

Figure 1. Specimen details

TABLE 1: DETAILS OF THE TEST SPECIMENS

No. of sample	Diameter (mm)	Thickness (mm)	Rein. wire mesh		Opening	Steel bars in each direction	Volume fraction %	Total weight of Rein. (kg)
			Type	No. of layers				
D1	1000	50	Welded	2	Without	Ø6 mm	1.0429	6.394
D2			Welded	2	With		1.048	6.385
D3		60	Fibreglass	2	Without		0.5471	5.367
D4			Polyethylene	1	Without		0.6237	6.119

In each dome, steel bars; 5 Ø 6 mm in the ring direction and 16 Ø 6 mm in the meridian direction were used as skeleton as shown in Figure 2. The first dome (D1) and the second dome (D2) were reinforced with two layers of welded galvanized wire meshes with 0.7 mm diameter and with 12.5x12.5 mm size of openings as shown in Figure 3. The properties of the used welded wire meshes were obtained from testing three samples using the Universal Testing Machine as shown in Figure 4. From the test results, the yield stress, ultimate stress and Modulus of elasticity can be considered as 400MPa, 600MPa and 170GPa; respectivily. Fiberglass mesh obtained from Gavazzi Company, Italy was used in reinforcements of the third dome (D3). Non-metal wire mesh made from high density polyethylene "Geogrid CE 121" was used in reinforcement the fourth dome (D4). The dimensions and properties of the fiberglass and polyethylene wire meshes as provided by producing companys are illustrated in Table 2 (refer to (26-29)).

The mortar mix was designed from Ordinary Portland Cement, fine aggregate sand with gradation presented in Table 3 and fresh drinking water and free from impurities. Silica fume with a powder form and with a gray color was used to replace part of the cement used by 10% by weight to obtain high strength mortar. The chemical composition of silica fume is given in Table 4. Polypropylene fiber (see Figure 3) by 900 gm/m^3 of the mortar mix and super plasticizer EDECRETE DM2, complies with ASTM C494-86 with specific weight of 1.05 at 20°c were used for the control of cracking due to drying shrinkage and thermal expansion/contraction, for decreasing concrete permeability, for increasing impact capacity, shatter resistance and abrasion. Chemical and physical properties of polypropylene fiber are shown in Table 5. The high range water reducing admixture (viscocrete-5930) obtained from Sika-Egypt Company for Construction was added to ferrocement mortar mix.

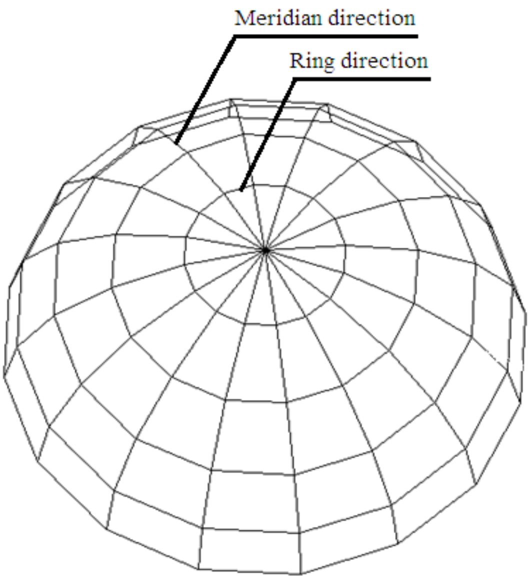

Figure 2. Skeleton bars

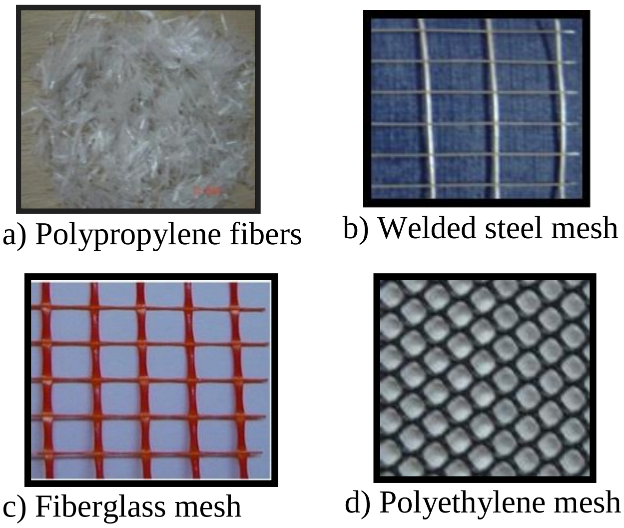

a) Polypropylene fibers
b) Welded steel mesh
c) Fiberglass mesh
d) Polyethylene mesh

Figure 3. Used fibers, reinforcement steel meshes and non-metallic mesh

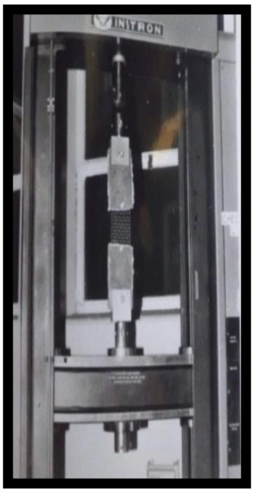

Figure 4. Wire mesh tensile test.

TABLE 2: TECHNICAL SPECIFICATION AND MECHANICAL PROPERTIES OF NON-METAL WIRE MESHES USED

			Fiberglass mesh	Polyethylene mesh
Dimension (mm)	Cross section	Longitudinal	1.66x0.66	3.3 (Diameter)
		Transverse	1.0x0.5	
	Opening dimensions		12.5x11.5	6x8
Properties	Weight (gm/m^2)		123	725
	Volume fraction (%)		0.535	2.04
	Tensile strength (MPa)		32.5	24.7
	Extension (%)		5.5	21

The mortar mix was designed according to the ACI recommendations [30] and the mix proportions by weight for mortar per cubic meter are presented in Table 6. Twelve 100 x 100 x 100 mm cubes were cast and tested after 7 and 28 days according to E.S.S [31] to estimate the compressive strength of the hardened mortar. Three cylinders 50 mm diameter and 100 mm length were laid horizontally in the Hydraulic Compression Testing Machine to determine the splitting tensile stress of the selected mortar mix after 28 days. The compression and tensile test results of the mortar mix are given in Table 7.

TABLE 3: SAND GRADATION.

Sieve Size (mm)	2.83	1.4	0.7	0.35	0.15
% Passing by weight	90.9	79	68	17	2
Limits of (E.E.S.)	100-85	100-75	80-60	30-10	10-0

TABLE 4: CHEMICAL COMOSITION OF SILICA FUME

Chemical	Weight percent (%)
SiO_2	92-94
Carbon	3-5
Fe_2O_3	0.1-0.5
CaO	0.1-0.15
AL_2O_3	0.2-0.3
MgO	0.1-0.2
MnO	0.008
K_2O	0.1
Na_2O	0.1

TABLE 5: CHEMICAL AND PHYSICAL PROPERTIES OF POLYPROPYLENE FIBERS

Absorption	Nil
Specific gravity	0.91
Fiber length	Single cut lengths
Electrical conductivity	Low
Acid & salt resistance	High
Melt point	324°F (162°C)
Thermal conductivity	Low
Ignition point	1100°F (593°C)
Alkali resistance	Alkali proof

TABLE 6: PROPORTIONS BY WEIGHT AND PROPORTIES OF THE FERROCEMENT MORTAR MIX.

Proportions		Properties		
Material	Weight (kg/m^3)	Compressive stress (MPa)	After 7 days	22
Cement	650		After 28 days	40
Sand	1310	Tensile strength (MPa)		4
Silica fume	10% replacement of cement content			
Water	230			
Superplasticizer	1.0% by weight of (cement+ silica fume)			

The four specimens were prepared in the following sequence:

1. The reinforcement of the dome was prepared at the first by forming the Skeleton bars as indicated in Figure 2. At the second the reinforcement is completed by adding the metal and non-metal wire meshes according the type of domes (see Table 1). The reinforcements are showed in Figure 5.
2. Fine aggregate and cement were firstly mixed together in dry state. After that 50% of the required water was added then adding the silica fume and fiber mesh 300-e3. After that the remaining 50% of the required water containing the admixture was added gradually. It takes about 10 minutes to give the required homogeneous mixtures.
3. The mortar was cast by plastering as shown in Figure 6.
4. The specimens were stripped 24 hours later and stored in the laboratory atmosphere until testing within 28 days. The specimens were covered using a wet cloth and water sprinkled twice a day.
5. Before testing, the faces of the specimen were painted in white to illustrate the form of cracks during the test.

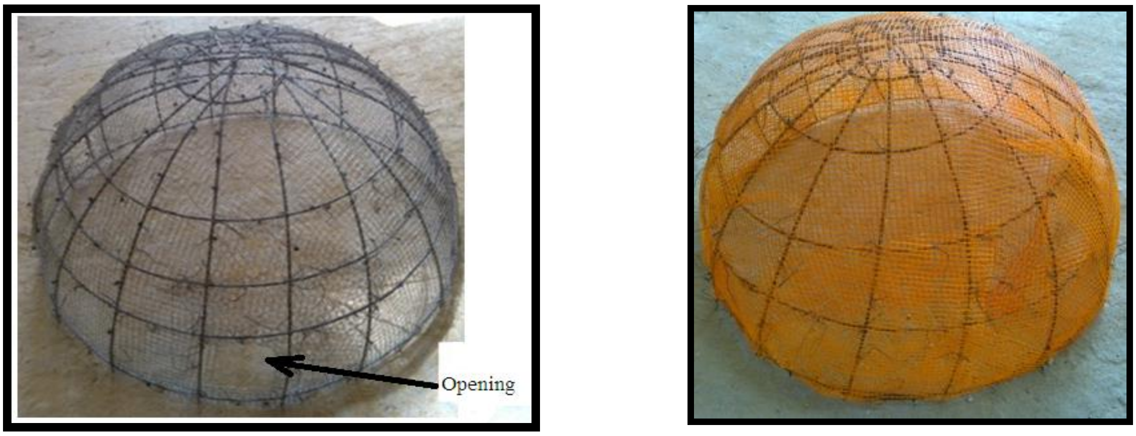

Figure 5. The reinforcements of specimens; a) D2 to the left b) D3 to the right

a) Partially plastering b) Finally plastering from out side

Figure 6. Plastering process of the fourth dome (D4) as the sample

A hydraulic jack (20 Ton capacity) was used for applying the loading at the center of the dome as shown in Figure 7. Load was applied at 5 kN increments. Three dial gauges with an accuracy of 0.01 mm were used to measure the horizontal and vertical displacements. The horizontal displacements were measured at two points (PH1&PH2) at distance 100 mm and 330 mm from the dome base while the vertical displacement was measured at the third point (PV1) at distance 390mm from the dome base as shown in Figure 8.

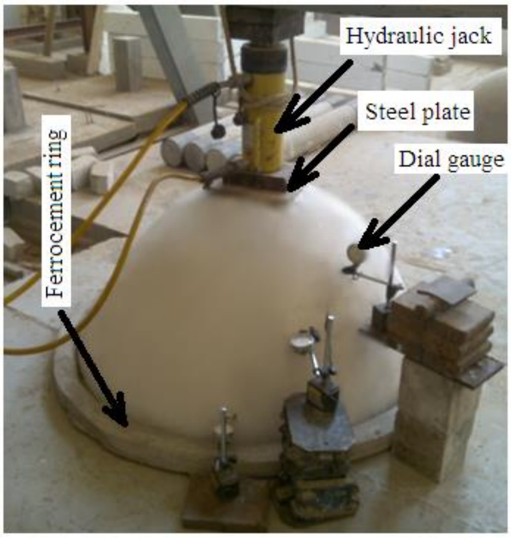

Figure 7. Specimen test

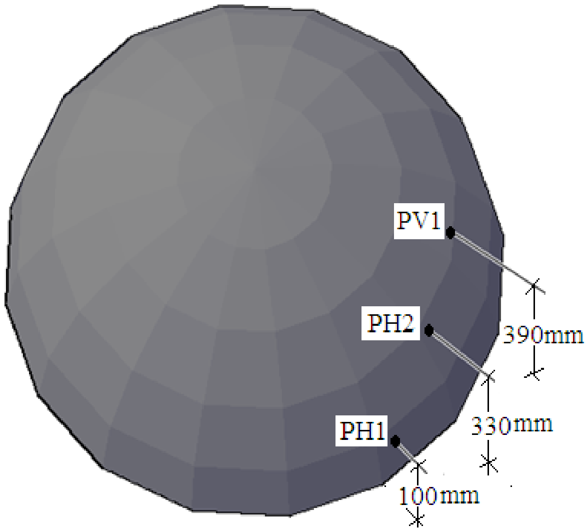

Figure 8. The measured displacement points

3. Finite Elements simulation

ANSYS computer program is utilized for analyzing structural components encountered throughout the current study. Three-dimensional brick element (Solid65 element) was used to simulate the mortar. Solid65 element has the capability of cracking in tension and crushing in compression. The element is defined by eight nodes having three degrees of freedom at each node: translations in the nodal x, y, and z directions. Up to three different rebar specifications may be defined. The rebar capability is available for modeling reinforcement behavior. Reinforcement is specified by its material, volume ratio and orientation angles. The volume ratio is defined as the rebar volume divided by the total element volume. The orientation is defined by two angles in degrees (θ and φ) from the element coordinate system (see Figure 9). Link8 element was used to simulate steel bars. The 3-D spar element (Link8 element) is a uniaxial tension-compression element with three degrees of freedom at each node: translations of the nodes in x, y, and z-directions. No bending moment is considered by using this element. Considering this element, plasticity, creep, swelling, stress stiffening, and large deflection capabilities can be considered in the analysis (32-35). The support is defined at all lower nodes as hinged support and the load was concentrated at seventeen nodes as seen in Figures 10 and 11.

In the current study, the domes were loaded up to failure so that the nonlinear material analysis was used. To model the plasticity of mortar in the program, the modulus of elasticity, poison's ratio, compressive and tensile strength after 28 days; they defined as obtained from the experimental work, and the relation between stress and strain of the mortar must be input. The modulus of elasticity and stress-strain curve of the mortar were employed the Egyptian Code [36]. The modulus of elasticity of concrete (E_c in MPa) was computed by Eq. (1) by considering the compressive strength of concrete after 28 days (F_{cu} in MPa). The multi-linear isotropic stress-strain curve for the concrete was calculated from Eq. (2). The calculated stress-strain curve for the used ferrocement mortar is presented in Figure 12 and the modulus of elasticity is considered as 27.8 GPa. The steel and the wire meshes (metal and non-metal) were defined by their yield stresses and the modulus of elasticity as pointed in the experimental work.

$$E_c = 4400\sqrt{F_{cu}} \qquad (1)$$

$$Stress = \frac{E_c \varepsilon}{1 + (\varepsilon/\varepsilon_0)^2} \qquad (2)$$

$$\varepsilon_0 = \frac{2F_{cu}}{E_c} \qquad (3)$$

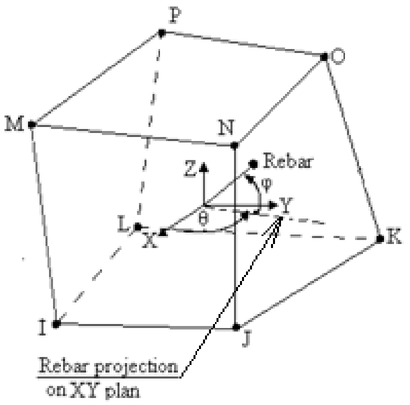

Figure 9. Solid65 element

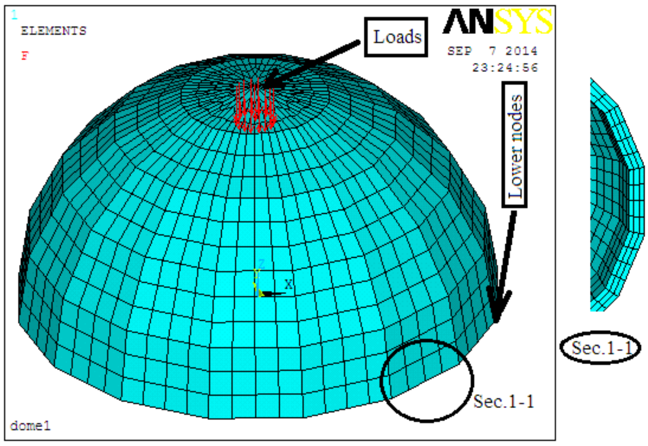

Figure 10. Finite element simulation for domes without opening

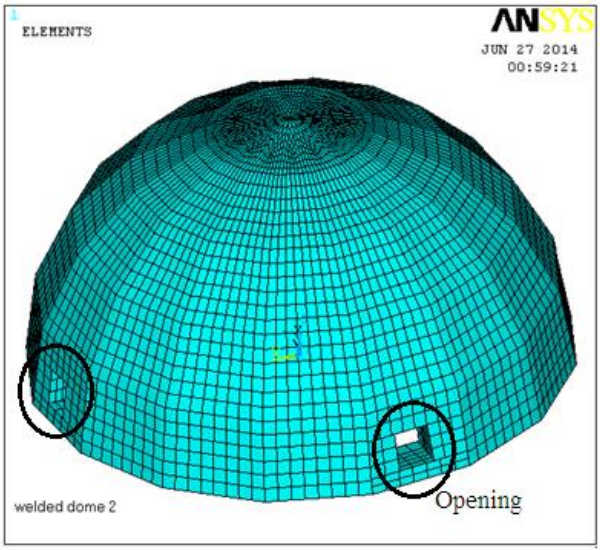

Figure 11. Finite element simulation for dome with opening

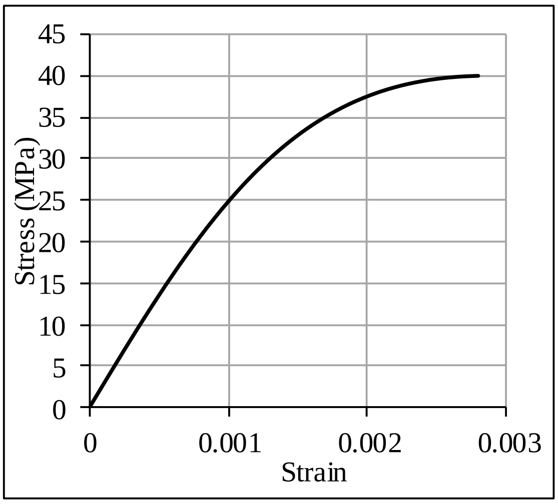

Figure 12. Stress-strain curve of ferrocement mortar

4. Results and discussions

The experimental results for the four domes included first crack load, ultimate load, service load, displacements at the first and ultimate load, ductility ratio and energy absorption were presented in Table 7. The energy absorption is calculated as the area under the load-deflection (vertical displacement) curve while Ductility ratio is defined in this investigation as the ratio between the vertical displacements at ultimate load to that at the first crack load. Service load (P_s), or flexural serviceability load, is defined as a function in the ultimate load (P_u) and the dead load (DL) of the dome; its own weight as shown in Eq. 4. Load-displacement curve at the three measured points are presented in Figure 13 to Figure 15 as obtained from the experimental tests.

$$P_s = \frac{P_u - 1.4DL}{1.6} \quad \dots\dots (4)$$

From the experimental results indicated in Table 7 and Figure 13 to Figure 15, it can be seen that specimen dome (D3) with two layers fiberglass mesh has the highest service load; 72.25kN and ultimate load; 120 kN. Also specimen dome D1 with two layer of welded wire meshes achieved highest ductility ratio: 1.9726% and energy absorption; 756 kN.mm. Additionally these results illustrated that the first crack appeared at the highest applied load in D4 (tested dome reinforced with one layer of polyethylene mesh) in the comparing with the other tested domes. On the other hand these results indicated that D4 has the lowest ductility ratio 1.4667% and energy absorption; 110 kN.mm. Also the ultimate load decreases in the fourth dome (D4) by 4.76% comparing with the first dome (D1).

The comparison between the results from the experimental work and FE simulations; load-vertical and horizontal displacements curves for the four specimens are presented in Figure 16 to Figure 26. From these Figures, it can be seen that the FE simulations for all tested beams give good results in comparing with the experimental results and the difference between the experimental and FE simulation results do not increase ~20%. The crack patterns of the four domes as obtained from the experimental and FE simulations are presented in Figure 27. From this figure it can be observed that the craks started in appearing under the applied load then these cracks were expanded towered the supports. Also these cracks increased in both of ferrocement dome with fiberglass and polyethylene mesh and the width of the cracks in these domes seem to be larger than in the domes with welded wire meshes.

TABLE 7: TEST RESULTS

NO. of sample	First crack load (kN)	Service load (kN)	Ultimate load (kN)	Displacement (mm) at the first crack			Displacement (mm) at the ultimate load			Ductility ratio (%)	Energy absorption (kN.mm)
				PH1	PH2	PV1	PH1	PH2	PV1		
D1	60	63.91	105	10.6	9.5	7.3	20	17.2	14.4	1.9726	756
D2	65	57.67	95	9.5	9.3	9	13.8	14.00	14	1.5556	665
D3	65	72.25	120	7.43	7.43	6.44	13.08	13.07	11.37	1.7655	682.2
D4	70	59.75	100	5.80	7.10	1.5	8.80	10.00	2.2	1.4667	110

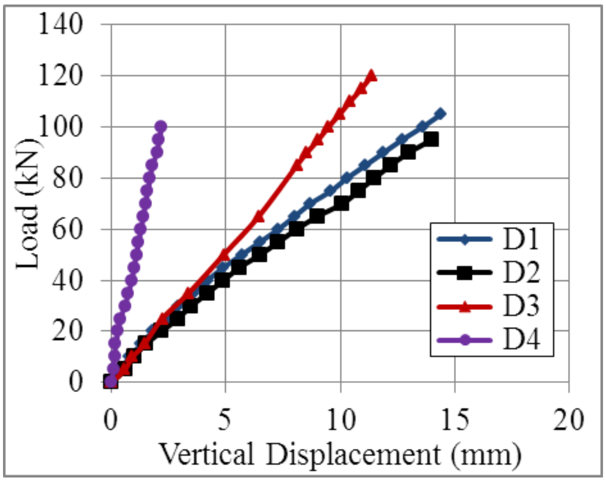

Figure 13. Experimental load-vertical displacement curve at PV1

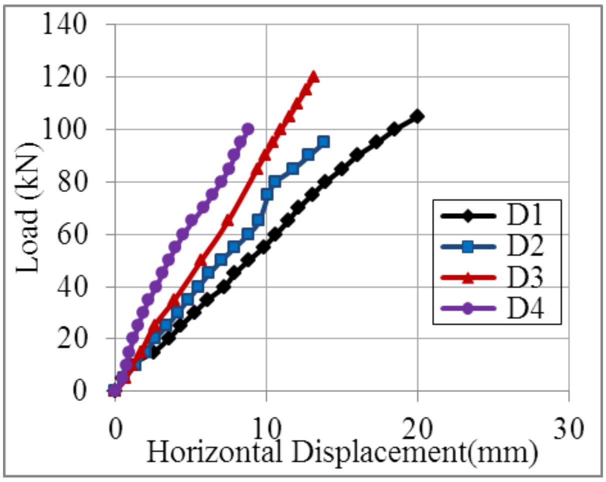

Figure 14. Experimental load-horizontal displacement curve at PH1

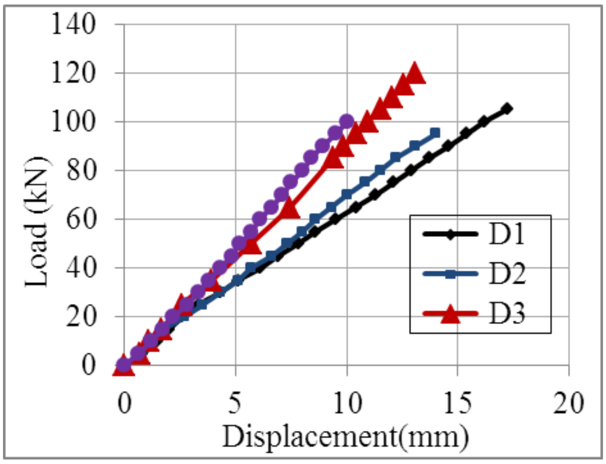

Figure 15. Experimental load-horizontal displacement curve at PH2

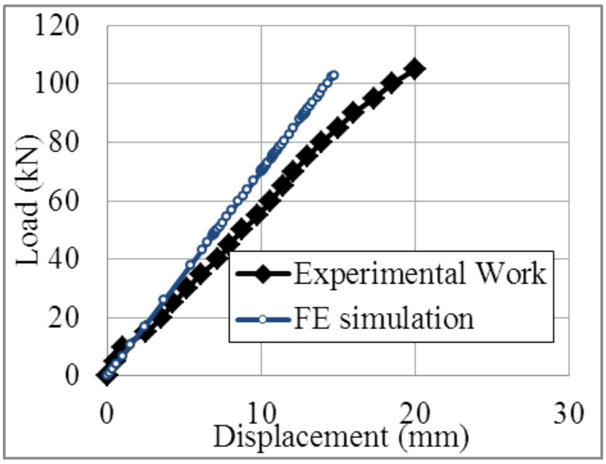

Figure 16. Experimental and numerical load-horizontal displacement curve at PH1 for D1

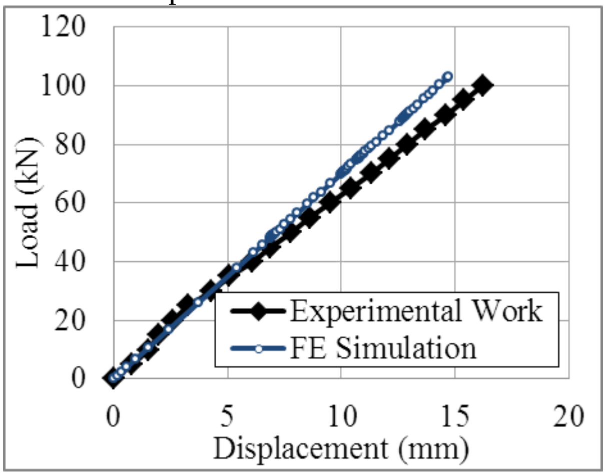

Figure 17. Experimental and numerical load-horizontal displacement curve at PH2 for D1

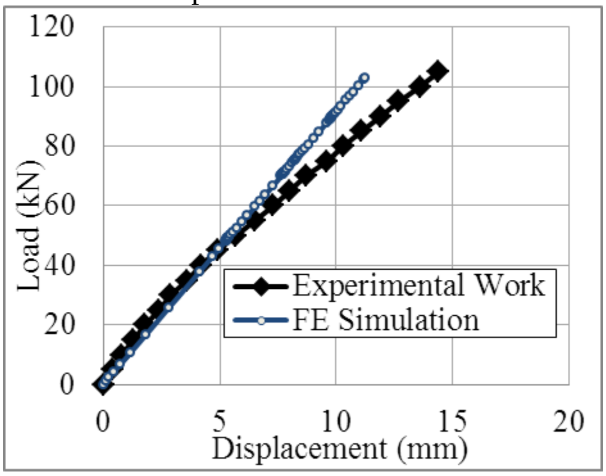

Figure 18. Experimental and numerical load-horizontal displacement curve at PV1 for D1

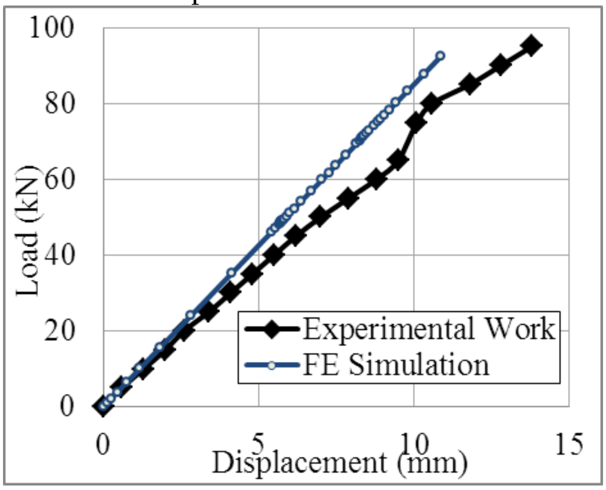

Figure 19. Experimental and numerical load-horizontal displacement curve at PH1 for D2

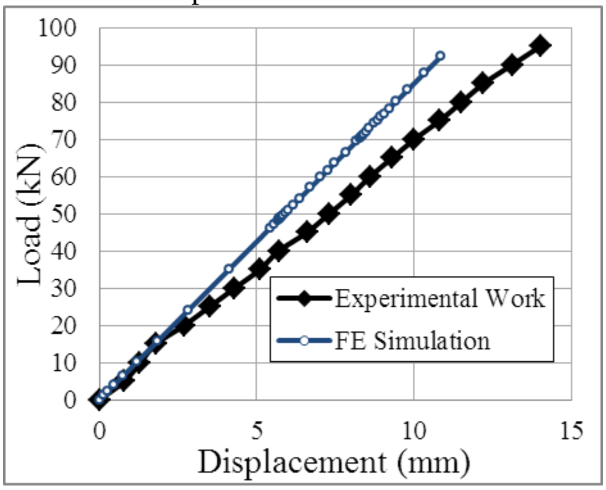

Figure 20. Experimental and numerical load-horizontal displacement curve at PH2 for D2

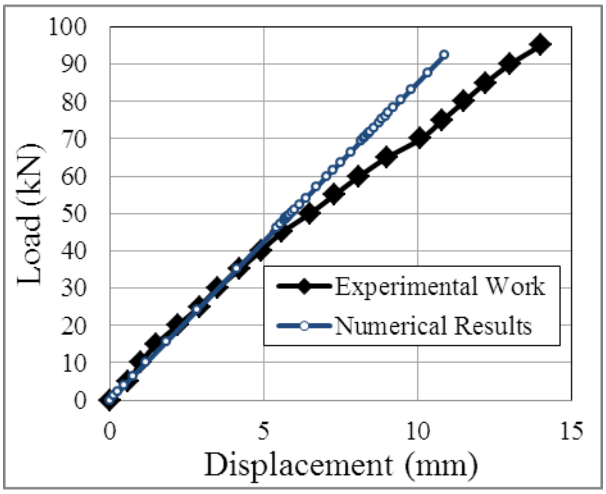

Figure 21. Experimental and numerical load-horizontal displacement curve at PV1 for D2

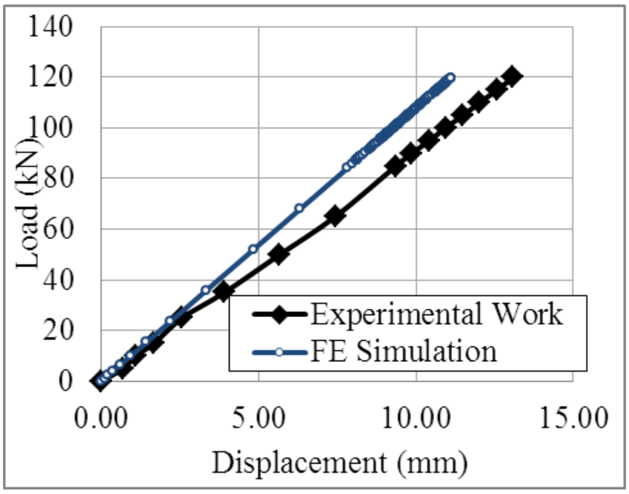

Figure 22. Experimental and numerical load-horizontal displacement curve at PH1 for D3

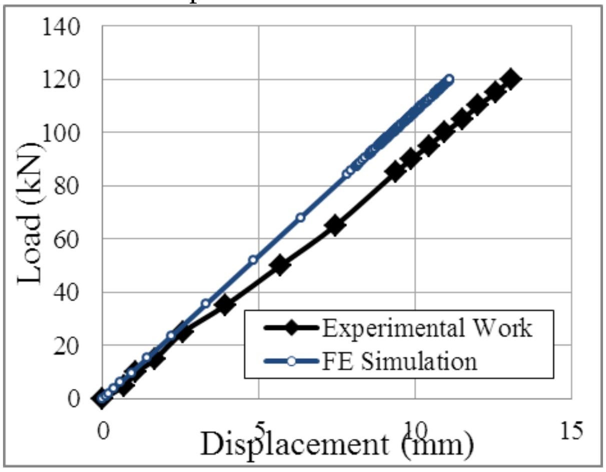

Figure 23. Experimental and numerical load-horizontal displacement curve at PH2 for D3

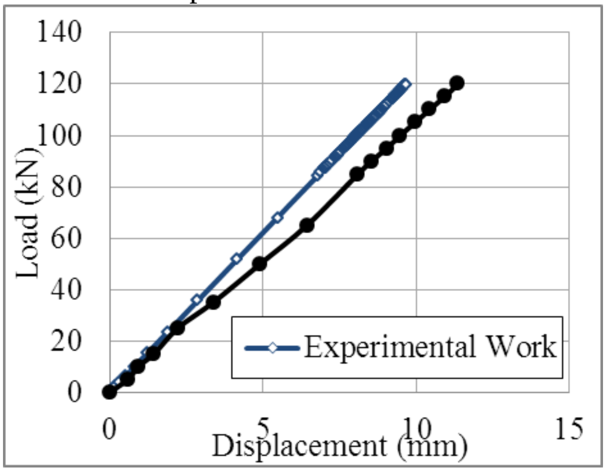

Figure 24. Experimental and numerical load-horizontal displacement curve at PV1 for D3

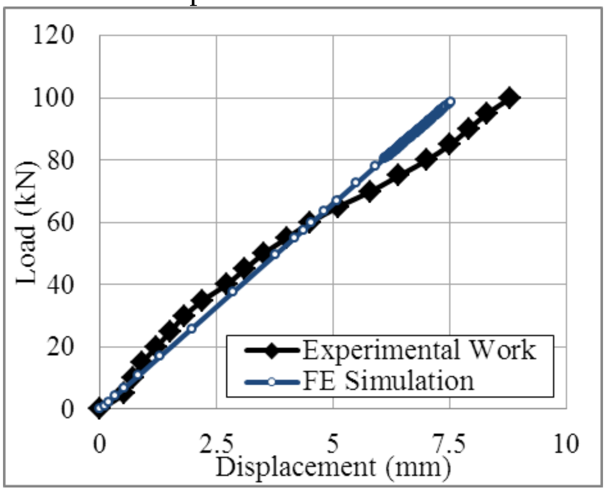

Figure 25. Experimental and numerical load-horizontal displacement curve at PH1 for D4

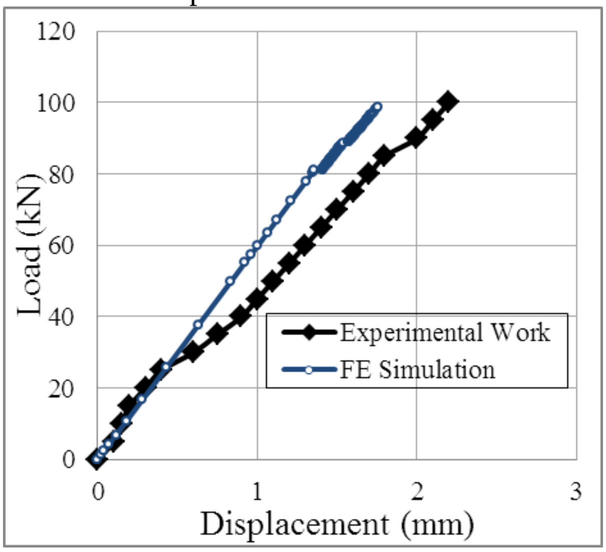

Figure 26. Experimental and numerical load-horizontal displacement curve at PV1 for D4

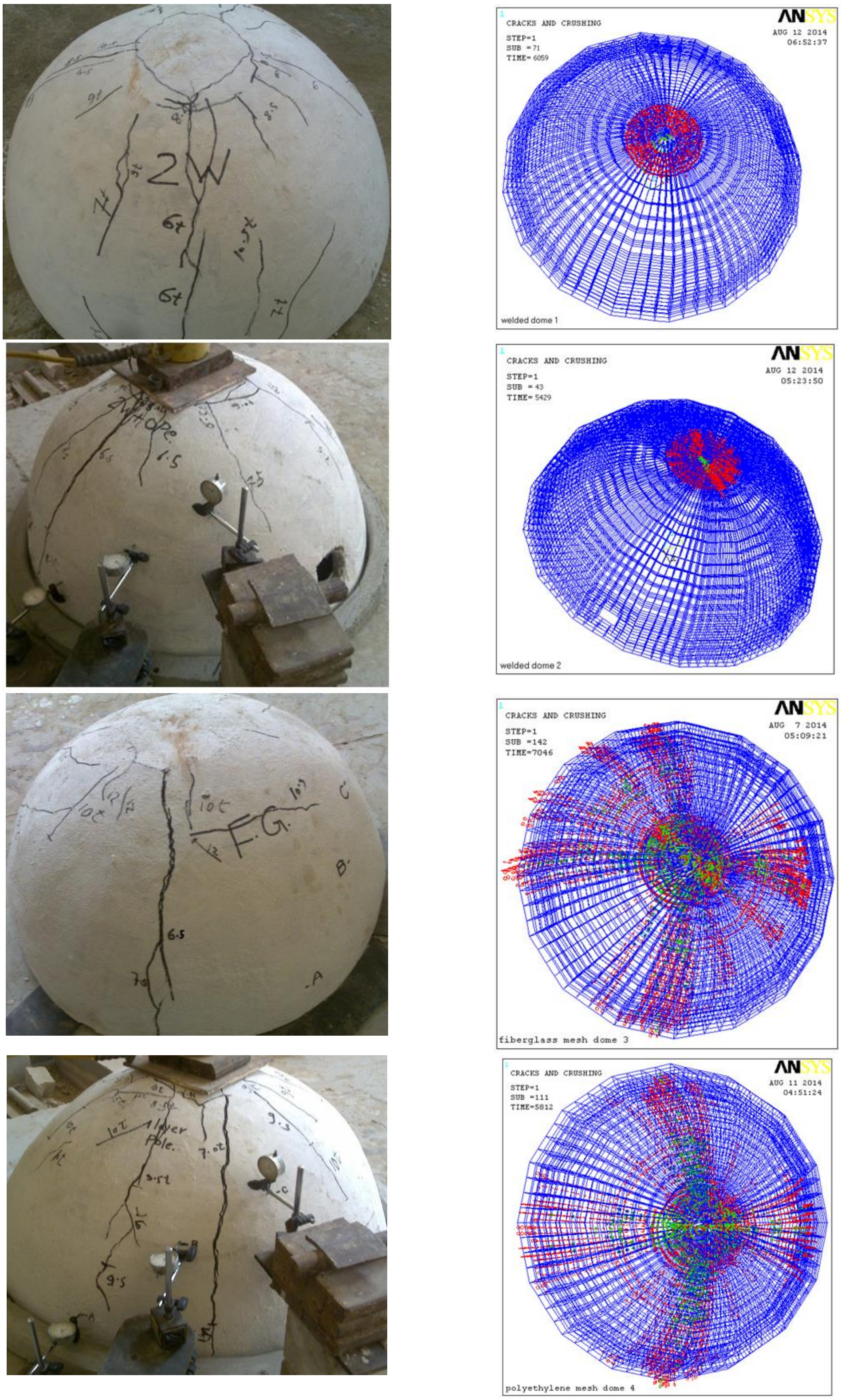

D1

D2

D3

D4

a) Experimental b) FE Simulation

Figure 27. Cracking patterns for all specimens

5. Conclusions

An experimental program was design to investigate the structural performance of the ferrocement reinforced with new composite materials. The traditional welded wire meshes were used as a reinforcement in the control dome and non-metallic wire meshes; fiberglass and polyethylene meshes were replaced the welded wire meshes in two specimens. Also the objective of the current paper is determining the effect of opening in the nonlinear behavior of the ferrocement dome. Four ferrocement domes were cast and tested up to failure and their results included the first crack load, service load, ultimate load, ductility ratio, energy absorption, the relationship between load and the vertical displacement, load-horizontal curve and the crack patterns are presented and discussed in the current work. Also FE simulations using ANSYS program were employed and their results were compared with the experimental results. Based on the experimental work and the numerical results presented in this research, the following conclusions can be drawn:

(1) Specimen dome reinforced with two layers of welded wire meshes achieved highest ductility ratio and energy absorption,

(2) The ferrocement dome reinforced with two layers of fiberglass mesh gave the highest failure load and service load. The ultimate load in this dome increased by ~14.28% than the control dome (the first dome with two layers of welded wire meshes),

(3) Tested dome reinforced with one layer of polyethylene mesh has the lowest ductility ratio and energy absorption.

(4) For the ferrocement dome with two opening, the ultimate load decreased with~9.5% while the energy absorption and the ductility ratio decreased by ~12% and ~21.12% respectively than the ultimate load in the control dome.

(5) The width of cracks increased by replacing the welded wire meshes by fiberglass meshes and polyethylene meshes.

(6) The employed finite element simulations of the ferrocement dome gave a good agreement with the experimental results.

References

1. Aboul-Anen, B., El-Shafey, A., and El-Shami, M., “Experimental and Analytical Model of Ferrocement Slabs,” International Journal of Recent Trends in Engineering, IJJCE, Oulu, Finland, 2009.
2. Ali, A., “Applications of Ferrocement as a Low Cost Construction Material in Malaysia,” Journal of Ferrocement, Vol. 25, No. 2, pp. 123-128, April, 1995.
3. Al-Kubaisy, M. A., and Jumaat, M. Z., “Flexural Behavior of Reinforced Concrete Slabs with Ferrocement Tension Zone Cover,” Journal of Construction and Building Materials, Vol. 14, pp. 245-252, 2000.
4. Robles-Austriaco, L., Pama, R. P., and Valls, J., “Ferrocement an Innovative Technology for Housing,” Journal of Ferrocement, Vol. 11, No. 1, pp. 23-47, 1981.
5. Elavenil, S., and Chandrasekar, V., “Analysis of Reinforced Concrete Beams Strengthened with Ferrocement,” International Journal of Applied Engineering Research,Vol. 2, No. 3, pp. 431-440, 2007.
6. Fahmy, E. H., Shaheen, Y. B., and Korany, Y. S., “Use of Ferrocement Laminates for Repairing Reinforced Concrete Slabs,” Journal of Ferrocement, Vol. 27, No. 3, pp. 219-232, July, 1997.
7. Jumaat, M., and Alam A., “Flexural Strengthening of Reinforced Concrete Beams Using Ferrocement Laminate with Skeletal Bars,” Journal of Applied Sciences Research, Vol. 2, No. 9, pp. 559-566, 2006.
8. Kaish, M. A., Alam, A. B., Jamil, M. R., Zain, M. F., Wahed, M. A., “Improved Ferrocement Jacketing for Restrengthening of Square RC Short Column,” Journal of Construction and Building Materials, Vol. 36,pp. 228–237, 2012.

9. Mourad, S. M., and Shannag, M. J., “Repair and Strengthening of Reinforced Concrete Square Columns Using Ferrocement Jackets,” Journal of Cement and Concrete Composites, Vol. 34, pp. 288–294, 2012.
10. Xiong, G. J., Wu, X. Y., Li, F.F., and Yan, Z. “Load Carrying Capacity and Ductility of Circular Concrete Columns Confined by Ferrocement Including Steel Bars,”Journal of Construction and Building Materials, Vol. 25, pp. 2263–2268, 2011.
11. El-Sakhawy, Y., “Structural Behavior of Ferrocement Roof Elements,” B. Sc. Thesis, Minufiya University, Shebin El-Kom, Egypt, 2000.
12. El-Halfawy, E., “Flexural Behavior of Ferrocement Deck Bridges,” M.Sc. thesis, Minufiya University, Shebin El-Kom, Egypt, 2003.
13. Shaheen, Y., Safan, M., and Abdalla, M., “Structural Behavior of Composite Reinforced Ferrocement Plates,” Journal of Concrete Research Letters, Vol. 4, No. 3, pp. 621-638, 2013.
14. Al-Rifaei, W. N., and Hassan, A. H., “Structural Behavior of Thin Ferrocement One-way Bending Elements,” Journal of Ferrocement, Vol. 24, No. 2, pp.115-126, 1994.
15. Wieland, M., “Analyses and Design of Shell Structures,” Short Course on Design and Construction of Ferrocement Structures, International Ferrocement Information Center, Bangkok, Thailand, 1985.
16. Jennings, P. J., “Unique Shape: Mosque Domes from Modern Techniques, Concrete International: Design and Construction,” Vol. 5, No. 11, pp. 41-45, 1983.
17. Elsakka, M. M., “Structural analysis of Ferrocement spherical domes,” Ph. D. Dissertation, Minufiya University, Shebin El-Kom, Egypt, 2012.
18. Al-Rifaie, W. N., and Azad A., “Experimental Investigation on Thin Ferrocement Dome Structures,” International Journal of Engineering and Advanced Technology, Vol. 3, No. 2, pp. 373-377, 2013.
19. Daniel, I., and Shah, P., “Fiber Reinforced Concrete, developments and innovations,” American Concrete Institute, SP-142, 1994.
20. Al-sayed, H., and Al-hozaimy, M., “Ductility of Concrete Beams Reinforced with FRP Bars and Steel Fibers,” Journal of Composite Material, Vol.33, No. 19, pp.1792–806, 1999.
21. Harris, G., Somboonsong, W., and Ko, K., “New Ductile Hybrid FRP Reinforcing Bar for Concrete Structures,” Journal of Composite Construction, Vol. 2, No.1, PP.28–37, 1998.
22. Li, C., and Wang, S., “Flexural Behaviors of Glass Fiber-Reinforced Polymer (GFRP) Reinforced Engineered Cementitious Composite Beams,” Journal of Material, Vol. 99, No. 1, PP. 11–21, 2002.
23. Qu, W., Zhang, X., and Huang, H., “Flexural behavior of concrete beams reinforced with hybrid (GFRP and steel) bars,” Journal of Composite Construction, Vol. 13, No. 5, 2009.
24. Sakthivel, P., and Jagannathan, A., “Study of Flexural Ferrocement and Thin Reinforced Cement Behavior of Ferrocement Slabs Reinforced with PVC-coated Weld Mesh,” International Journal of Engineering Research and Development, Vol. 1, No. 12, pp. 50-57, 2012.
25. Sakthivel, P., and Jagannathan, A., “Fibrous Ferrocement Composite with PVC-coated Weld Mesh and Bar-chip Polyolefin Fibers,” International Journal of EOMATE, Vol. 3, No. 2, pp. 381-388, 2012.
26. Hafiz, A., “Structural Behaviour of Ferrocement channels Beams,” M. Sc. thesis, Minufiya University, Shebin El-Kom, Egypt, 2012.

27. Shaheen,Y., Soliman, N., and. Hafiz, A., “Structural Behavior of Ferrocement channels Beams,” Journal of Concrete research Letters, Vol. 4, No. 3, pp. 621-638. 2013.
28. Abdul-Fataha S., “Structural Behavior of Concrete Beams Reinforced with Innovative Materials,” M. Sc. thesis, Minufiya University, Shebin El-Kom, Egypt, 2014.
29. Shaheen, Y. Eltaly B. and Abdul-Fataha S., “Structural Performance of Ferrocement Beams Reinforced with Composite Materials,” Structural Engineering and Mechanics, Vol. 50, No. 6, PP. 817-834, 2014.
30. State-of-the-Art Report on Ferrocement, Reported by ACI Committee 549, 1980.
31. E.S.S “Egyptian Standard Specifications for Plain and Reinforcement Concrete,” Egypt, No. 2070-2007, 2011.
32. ANSYS, “Help and Manual,” 12th Editor, ANSYS Inc, PA, USA, 2006.
33. Hoque, M., “3D Nonlinear Mixed Finite-element Analysis of RC Beams and Plates with and without FRP Reinforcement,” M. Sc. Thesis, University of Manitoba, Winnipeg, Manitoba, Canada, 2006.
34. Singh, G., “Finite Element Analysis of Reinforced Concrete Shear Walls,” M. Sc. Thesis, Deemed University, India, 2006.
35. Shaheen, Y. B. I., Eltaly, B. and Kameel, M., “Experimental and Analytical Investigation of Ferrocement Water Pipe,” Journal of Civil Engineering and Construction Technolog, Vol. 4, No. 4, pp. 157-167, May, 2013.
36. E.C.P. “Egyptian code of practice: design and construction for reinforced concrete structures,” Research Centre for Houses Building and Physical Planning, Cairo, Egypt, No. 203, 2007.